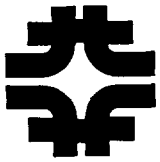

Fermi National Accelerator Laboratory

FERMILAB-Pub-96/317-E
CDF

Measurement of Dijet Angular Distributions at CDF

F. Abe et al.
The CDF Collaboration

Fermi National Accelerator Laboratory
P.O. Box 500, Batavia, Illinois 60510

September 1996

Submitted to *Physical Review Letters*

Disclaimer

Distribution

CDF/PUB/JET/PUBLIC/3773
FERMILAB-PUB-96/317-E

Measurement of Dijet Angular Distributions at CDF

F. Abe,[15] H. Akimoto,[34] A. Akopian,[29] M. G. Albrow,[7] S. R. Amendolia,[25] D. Amidei,[18] J. Antos,[31] C. Anway-Wiese,[4] S. Aota,[34] G. Apollinari,[29] T. Arisawa,[34] T. Asakawa,[34] W. Ashmanskas,[16] M. Atac,[7] F. Azfar,[24] P. Azzi-Bacchetta,[23] N. Bacchetta,[23] W. Badgett,[18] S. Bagdasarov,[29] M. W. Bailey,[20] J. Bao,[37] P. de Barbaro,[28] A. Barbaro-Galtieri,[16] V. E. Barnes,[27] B. A. Barnett,[14] E. Barzi,[8] G. Bauer,[17] T. Baumann,[10] F. Bedeschi,[25] S. Behrends,[3] S. Belforte,[25] G. Bellettini,[25] J. Bellinger,[36] D. Benjamin,[33] J. Benlloch,[17] J. Bensinger,[3] D. Benton,[24] A. Beretvas,[7] J. P. Berge,[7] J. Berryhill,[5] S. Bertolucci,[8] B. Bevensee,[24] A. Bhatti,[29] K. Biery,[13] M. Binkley,[7] D. Bisello,[23] R. E. Blair,[1] C. Blocker,[3] A. Bodek,[28] W. Bokhari,[17] V. Bolognesi,[2] G. Bolla,[23] D. Bortoletto,[27] J. Boudreau,[26] L. Breccia,[2] C. Bromberg,[19] N. Bruner,[20] E. Buckley-Geer,[7] H. S. Budd,[28] K. Burkett,[18] G. Busetto,[23] A. Byon-Wagner,[7] K. L. Byrum,[1] J. Cammerata,[14] C. Campagnari,[7] M. Campbell,[18] A. Caner,[25] W. Carithers,[16] D. Carlsmith,[36] A. Castro,[23] D. Cauz,[25] Y. Cen,[28] F. Cervelli,[25] P. S. Chang,[31] P. T. Chang,[31] H. Y. Chao,[31] J. Chapman,[18] M. -T. Cheng,[31] G. Chiarelli,[25] T. Chikamatsu,[34] C. N. Chiou,[31] L. Christofek,[12] S. Cihangir,[7] A. G. Clark,[9] M. Cobal,[25] E. Cocca,[25] M. Contreras,[5] J. Conway,[30] J. Cooper,[7] M. Cordelli,[8] C. Couyoumtzelis,[9] D. Crane,[1] D. Cronin-Hennessy,[6] R. Culbertson,[5] T. Daniels,[17] F. DeJongh,[7] S. Delchamps,[7] S. Dell'Agnello,[25] M. Dell'Orso,[25] R. Demina,[7] L. Demortier,[29] B. Denby,[25] M. Deninno,[2] P. F. Derwent,[7] T. Devlin,[30] J. R. Dittmann,[6] S. Donati,[25] J. Done,[32] T. Dorigo,[23] A. Dunn,[18] N. Eddy,[18] K. Einsweiler,[16] J. E. Elias,[7] R. Ely,[16] E. Engels, Jr.,[26] D. Errede,[12] S. Errede,[12] Q. Fan,[27] C. Ferretti,[25] I. Fiori,[2] B. Flaugher,[7] L. Fortney,[6] G. W. Foster,[7] M. Franklin,[10] M. Frautschi,[33] J. Freeman,[7] J. Friedman,[17] H. Frisch,[5] T. A. Fuess,[1] Y. Fukui,[15] S. Funaki,[34] G. Gagliardi,[25] S. Galeotti,[25] M. Gallinaro,[23] M. Garcia-Sciveres,[16] A. F. Garfinkel,[27] C. Gay,[10] S. Geer,[7] D. W. Gerdes,[14] P. Giannetti,[25] N. Giokaris,[29] P. Giromini,[8] G. Giusti,[25] L. Gladney,[24] D. Glenzinski,[14] M. Gold,[20] J. Gonzalez,[24] A. Gordon,[10] A. T. Goshaw,[6] K. Goulianos,[29] H. Grassmann,[25] L. Groer,[30] C. Grosso-Pilcher,[5] G. Guillian,[18] R. S. Guo,[31] C. Haber,[16] E. Hafen,[17] S. R. Hahn,[7] R. Hamilton,[10] R. Handler,[36] R. M. Hans,[37] K. Hara,[34] A. D. Hardman,[27] B. Harral,[24] R. M. Harris,[7] S. A. Hauger,[6] J. Hauser,[4] C. Hawk,[30] E. Hayashi,[34] J. Heinrich,[24] K. D. Hoffman,[27] M. Hohlmann,[5] C. Holck,[24] R. Hollebeek,[24] L. Holloway,[12] A. Hölscher,[13] S. Hong,[18] G. Houk,[24] P. Hu,[26] B. T. Huffman,[26] R. Hughes,[21] J. Huston,[19] J. Huth,[10] J. Hylen,[7] H. Ikeda,[34] M. Incagli,[25] J. Incandela,[7] G. Introzzi,[25] J. Iwai,[34] Y. Iwata,[11] H. Jensen,[7] U. Joshi,[7] R. W. Kadel,[16] E. Kajfasz,[23] H. Kambara,[9] T. Kamon,[32] T. Kaneko,[34] K. Karr,[35] H. Kasha,[37] Y. Kato,[22] T. A. Keaffaber,[27] L. Keeble,[8] K. Kelley,[17] R. D. Kennedy,[30] R. Kephart,[7] P. Kesten,[16] D. Kestenbaum,[10] R. M. Keup,[12] H. Keutelian,[7] F. Keyvan,[4] B. Kharadia,[12] B. J. Kim,[28] D. H. Kim,[7a] H. S. Kim,[13] S. B. Kim,[18] S. H. Kim,[34] Y. K. Kim,[16] L. Kirsch,[3] P. Koehn,[28] K. Kondo,[34] J. Konigsberg,[10] S. Kopp,[5] K. Kordas,[13]

Submitted to Physical Review Letters September 17, 1996

A. Korytov,[17] W. Koska,[7] E. Kovacs,[7a] W. Kowald,[6] M. Krasberg,[18] J. Kroll,[7] M. Kruse,[28] T. Kuwabara,[34] S. E. Kuhlmann,[1] E. Kuns,[30] A. T. Laasanen,[27] N. Labanca,[25] S. Lammel,[7] J. I. Lamoureux,[3] T. LeCompte,[1] S. Leone,[25] J. D. Lewis,[7] P. Limon,[7] M. Lindgren,[4] T. M. Liss,[12] N. Lockyer,[24] O. Long,[24] C. Loomis,[30] M. Loreti,[23] J. Lu,[32] D. Lucchesi,[25] P. Lukens,[7] S. Lusin,[36] J. Lys,[16] K. Maeshima,[7] A. Maghakian,[29] P. Maksimovic,[17] M. Mangano,[25] J. Mansour,[19] M. Mariotti,[23] J. P. Marriner,[7] A. Martin,[12] J. A. J. Matthews,[20] R. Mattingly,[17] P. McIntyre,[32] P. Melese,[29] A. Menzione,[25] E. Meschi,[25] S. Metzler,[24] C. Miao,[18] T. Miao,[7] G. Michail,[10] R. Miller,[19] H. Minato,[34] S. Miscetti,[8] M. Mishina,[15] H. Mitsushio,[34] T. Miyamoto,[34] S. Miyashita,[34] N. Moggi,[25] Y. Morita,[15] J. Mueller,[26] A. Mukherjee,[7] T. Muller,[4] P. Murat,[25] H. Nakada,[34] I. Nakano,[34] C. Nelson,[7] D. Neuberger,[4] C. Newman-Holmes,[7] M. Ninomiya,[34] L. Nodulman,[1] S. H. Oh,[6] K. E. Ohl,[37] T. Ohmoto,[11] T. Ohsugi,[11] R. Oishi,[34] M. Okabe,[34] T. Okusawa,[22] R. Oliveira,[24] J. Olsen,[36] C. Pagliarone,[2] R. Paoletti,[25] V. Papadimitriou,[33] S. P. Pappas,[37] N. Parashar,[25] S. Park,[7] A. Parri,[8] J. Patrick,[7] G. Pauletta,[25] M. Paulini,[16] A. Perazzo,[25] L. Pescara,[23] M. D. Peters,[16] T. J. Phillips,[6] G. Piacentino,[2] M. Pillai,[28] K. T. Pitts,[7] R. Plunkett,[7] L. Pondrom,[36] J. Proudfoot,[1] F. Ptohos,[10] G. Punzi,[25] K. Ragan,[13] D. Reher,[16] A. Ribon,[23] F. Rimondi,[2] L. Ristori,[25] W. J. Robertson,[6] T. Rodrigo,[25] S. Rolli,[25] J. Romano,[5] L. Rosenson,[17] R. Roser,[12] W. K. Sakumoto,[28] D. Saltzberg,[5] A. Sansoni,[8] L. Santi,[25] H. Sato,[34] P. Schlabach,[7] E. E. Schmidt,[7] M. P. Schmidt,[37] A. Scribano,[25] S. Segler,[7] S. Seidel,[20] Y. Seiya,[34] G. Sganos,[13] M. D. Shapiro,[16] N. M. Shaw,[27] Q. Shen,[27] P. F. Shepard,[26] M. Shimojima,[34] M. Shochet,[5] J. Siegrist,[16] A. Sill,[33] P. Sinervo,[13] P. Singh,[26] J. Skarha,[14] K. Sliwa,[35] F. D. Snider,[14] T. Song,[18] J. Spalding,[7] T. Speer,[9] P. Sphicas,[17] F. Spinella,[25] M. Spiropulu,[10] L. Spiegel,[7] L. Stanco,[23] J. Steele,[36] A. Stefanini,[25] K. Strahl,[13] J. Strait,[7] R. Ströhmer,[7a] D. Stuart,[7] G. Sullivan,[5] A. Soumarokov,[31] K. Sumorok,[17] J. Suzuki,[34] T. Takada,[34] T. Takahashi,[22] T. Takano,[34] K. Takikawa,[34] N. Tamura,[11] F. Tartarelli,[25] W. Taylor,[13] P. K. Teng,[31] Y. Teramoto,[22] S. Tether,[17] D. Theriot,[7] T. L. Thomas,[20] R. Thun,[18] M. Timko,[35] P. Tipton,[28] A. Titov,[29] S. Tkaczyk,[7] D. Toback,[5] K. Tollefson,[28] A. Tollestrup,[7] J. F. de Troconiz,[10] S. Truitt,[18] J. Tseng,[14] N. Turini,[25] T. Uchida,[34] N. Uemura,[34] F. Ukegawa,[24] G. Unal,[24] J. Valls,[7a] S. C. van den Brink,[26] S. Vejcik, III,[18] G. Velev,[25] R. Vidal,[7] M. Vondracek,[12] D. Vucinic,[17] R. G. Wagner,[1] R. L. Wagner,[7] J. Wahl,[5] N. Wallace,[25] C. Wang,[6] C. H. Wang,[31] J. Wang,[5] M. J. Wang,[31] Q. F. Wang,[29] A. Warburton,[13] T. Watts,[30] R. Webb,[32] C. Wei,[6] C. Wendt,[36] H. Wenzel,[16] W. C. Wester, III,[7] A. B. Wicklund,[1] E. Wicklund,[7] R. Wilkinson,[24] H. H. Williams,[24] P. Wilson,[5] B. L. Winer,[21] D. Winn,[18] D. Wolinski,[18] J. Wolinski,[19] S. Worm,[20] X. Wu,[9] J. Wyss,[23] A. Yagil,[7] W. Yao,[16] K. Yasuoka,[34] Y. Ye,[13] G. P. Yeh,[7] P. Yeh,[31] M. Yin,[6] J. Yoh,[7] C. Yosef,[19] T. Yoshida,[22] D. Yovanovitch,[7] I. Yu,[7] L. Yu,[20] J. C. Yun,[7] A. Zanetti,[25] F. Zetti,[25] L. Zhang,[36] W. Zhang,[24] and S. Zucchelli[2]

(CDF Collaboration)

[1] *Argonne National Laboratory, Argonne, Illinois 60439*

[2] *Istituto Nazionale di Fisica Nucleare, University of Bologna, I-40126 Bologna, Italy*

[3] *Brandeis University, Waltham, Massachusetts 02254*

[4] *University of California at Los Angeles, Los Angeles, California 90024*

[5] *University of Chicago, Chicago, Illinois 60637*

[6] *Duke University, Durham, North Carolina 27708*

[7] *Fermi National Accelerator Laboratory, Batavia, Illinois 60510*

[8] *Laboratori Nazionali di Frascati, Istituto Nazionale di Fisica Nucleare, I-00044 Frascati, Italy*

[9] *University of Geneva, CH-1211 Geneva 4, Switzerland*

[10] *Harvard University, Cambridge, Massachusetts 02138*

[11] *Hiroshima University, Higashi-Hiroshima 724, Japan*

[12] *University of Illinois, Urbana, Illinois 61801*

[13] *Institute of Particle Physics, McGill University, Montreal H3A 2T8, and University of Toronto, Toronto M5S 1A7, Canada*

[14] *The Johns Hopkins University, Baltimore, Maryland 21218*

[15] *National Laboratory for High Energy Physics (KEK), Tsukuba, Ibaraki 305, Japan*

[16] *Ernest Orlando Lawrence Berkeley National Laboratory, Berkeley, California 94720*

[17] *Massachusetts Institute of Technology, Cambridge, Massachusetts 02139*

[18] *University of Michigan, Ann Arbor, Michigan 48109*

[19] *Michigan State University, East Lansing, Michigan 48824*

[20] *University of New Mexico, Albuquerque, New Mexico 87131*

[21] *The Ohio State University, Columbus, OH 43210*

[22] *Osaka City University, Osaka 588, Japan*

[23] *Universita di Padova, Istituto Nazionale di Fisica Nucleare, Sezione di Padova, I-35131 Padova, Italy*

[24] *University of Pennsylvania, Philadelphia, Pennsylvania 19104*

[25] *Istituto Nazionale di Fisica Nucleare, University and Scuola Normale Superiore of Pisa, I-56100 Pisa, Italy*

[26] *University of Pittsburgh, Pittsburgh, Pennsylvania 15260*

[27] *Purdue University, West Lafayette, Indiana 47907*

[28] *University of Rochester, Rochester, New York 14627*

[29] *Rockefeller University, New York, New York 10021*

[30] *Rutgers University, Piscataway, New Jersey 08854*

[31] *Academia Sinica, Taipei, Taiwan 11529, Republic of China*

[32] *Texas A&M University, College Station, Texas 77843*

[33] *Texas Tech University, Lubbock, Texas 79409*

[34] *University of Tsukuba, Tsukuba, Ibaraki 305, Japan*

[35] *Tufts University, Medford, Massachusetts 02155*

[36] *University of Wisconsin, Madison, Wisconsin 53706*

[37] *Yale University, New Haven, Connecticut 06511*

Abstract

We have used 106 pb^{-1} of data collected in $p\bar{p}$ collisions at $\sqrt{s} = 1.8$ TeV by the Collider Detector at Fermilab to measure jet angular distributions in events with two jets in the final state. The angular distributions agree with next to leading order (NLO) predictions of Quantum Chromodynamics (QCD) in all dijet invariant mass regions. The data exclude at 95% confidence level (CL) a model of quark substructure in which only up and down quarks are composite and the contact interaction scale is $\Lambda^+_{ud} \leq 1.6$ TeV or $\Lambda^-_{ud} \leq 1.4$ TeV. For a model in which all quarks are composite the excluded regions are $\Lambda^+ \leq 1.8$ TeV and $\Lambda^- \leq 1.6$ TeV.

PACS numbers: 13.87.Ce, 12.38.Qk, 12.50.Ch, 13.85.Ni

Hard collisions between protons and antiprotons predominantly produce events containing two high energy jets (dijets). Measurement of the distribution of the scattering angle, between the dijet and the proton beam in the dijet center of mass frame, can provide a fundamental test of QCD and a sensitive probe of new physics. Dijet angular distributions reflect the dynamics of the hard scattering of quarks and gluons, and are expected to be fairly insensitive to the momentum distributions of these partons within the proton. As in Rutherford scattering, dijet angular distributions from QCD processes are peaked in the forward direction. In contrast, many

sources of new physics produce more isotropic dijet angular distributions. Our previous measurements using 4.2 pb^{-1} of data found the dijet angular distributions to be in good agreement with QCD predictions [1], and excluded a compositeness scale $\Lambda^{+}_{ud} < 1.0$ TeV for a contact interaction associated with compositeness of up and down quarks [2]. Here we report a measurement with a data sample that is 25 times larger.

We are also motivated by the observation that the inclusive differential jet cross section is above a QCD prediction at high transverse energy, E_T [3]. Interpretations of this high-E_T jet excess vary from explanations within the Standard Model (modifications of the parton distributions [4, 5] or QCD corrections [6]) to explanations beyond the Standard Model (e.g. quark compositeness [2], excited quarks [7], new Z bosons [8], new massive gluons [9], light gluinos [10], and anomalous chromomagnetic moments of quarks [11]). Measurements of the dijet angular distributions can help in resolving whether the measured excess of events with high E_T jets is a signal of new physics or merely new information on the ingredients of QCD calculations.

A detailed description of the Collider Detector at Fermilab (CDF) can be found elsewhere [12]. We use a coordinate system with z along the proton beam direction, transverse coordinate perpendicular to the beam, azimuthal angle ϕ, polar angle θ, and pseudorapidity $\eta = -\ln\tan(\theta/2)$. Jets are identified as localized energy depositions in the CDF calorimeters, which are constructed in a tower geometry. The jet axis is defined as the centroid in (η,ϕ) space of the calorimeter tower transverse

energies inside a radius $R = \sqrt{(\Delta\eta)^2 + (\Delta\phi)^2} = 0.7$ of the axis. The jet energy, E, and momentum, $\vec{P}$, are defined as the scalar and vector sums, respectively, of the tower energies inside this radius. E and $\vec{P}$ are corrected for non-linearities in the calorimeter response, energy lost in uninstrumented regions and outside the clustering cone, and energy gained from the underlying event and multiple interactions. The jet energy corrections increase the reconstructed jet energies on average by 24%(19%) for 50 GeV (500 GeV) jets. Details of jet reconstruction and jet energy corrections can be found elsewhere [13].

The dijet system consists of the two jets with the highest transverse momentum in the event (leading jets). We measure inclusive dijet events, defined as $p\bar{p} \rightarrow$ 2 leading jets + X, where X can be anything, including additional jets. The dijet invariant mass is defined as $M = \sqrt{(E_1 + E_2)^2 - (\vec{P}_1 + \vec{P}_2)^2}$. We use the dijet angular variable $\chi = \exp(|\eta_1 - \eta_2|)$, where η_1 and η_2 are the pseudorapidities of the two leading jets. The variable χ has the benefit of only containing angular quantities, and hence is more accurately measured than a variable that involves the absolute jet energy. For the case of $2 \rightarrow 2$ parton scattering, χ is related to the scattering angle in the center of mass frame, θ^*, by $\chi = (1+|\cos\theta^*|)/(1-|\cos\theta^*|)$. The χ distribution of QCD produced jets is roughly flat while many models of quark compositeness give angular distributions that are strongly peaked at low χ. To select events with high trigger efficiency and to avoid problematic regions of the detector, this analysis requires $\chi < 5$, $|\eta_1| < 2$, and $|\eta_2| < 2$. To characterize the shape of the angular distribution in a mass bin with a

single number, we use the variable $R_\chi = N(\chi < 2.5)/N(2.5 < \chi < 5)$, the ratio of the number of dijet events with $\chi < 2.5$ to the number of dijet events with $2.5 < \chi < 5$. Isotropic angular distributions and contact interactions both tend to produce more events in the region $\chi < 2.5$ than QCD, and hence will have a higher value of R_χ. The pivot point $\chi = 2.5$ was chosen to optimize the sensitivity to a left-handed contact interaction [2].

Our data sample was obtained in the 1992-95 running periods using four single-jet triggers with thresholds on the uncorrected cluster transverse energies of 20, 50, 70, and 100 GeV. After applying the jet energy corrections the last three trigger samples were used to measure the dijet angular distribution in mass bins above 241, 300, and 400 GeV/c^2, respectively. At these mass thresholds the trigger efficiencies were greater than 95% at all values of χ considered; the average efficiency was greater than 99% in each mass bin. The 20 GeV trigger sample was only used to measure the trigger efficiency of the 50 GeV sample. The four data samples corresponded to integrated luminosities of 0.126, 2.84, 14.1, and 106 pb^{-1}. To utilize the projective nature of the calorimeter towers, the z position of the event vertex was required to be within 60 cm of the center of the detector; this cut removed 7% of the events. Backgrounds from cosmic rays, beam halo, and detector noise were removed with the cuts reported previously [14], and residual backgrounds were removed by requiring that the total observed energy be less than 2 TeV.

The raw χ distribution was measured in five bins of dijet mass: $241 < M < 300$, $300 < M < 400$, $400 < M < 517$, $517 < M < 625$, and $M > 625$ GeV/c^2. Variations

in the jet response and energy resolution of the calorimeter as a function of detector η produced distortions in the measured angular distribution. To understand and correct for this effect a parametrized Monte Carlo program was developed that modeled in detail the measured jet response of the CDF detector after the application of the standard jet corrections. The relative jet response was determined from conservation of transverse momentum, P_T, by requiring a jet in the region $0.15 < |\eta| < 0.9$ and measuring the relative response of a jet in another pseudorapidity region (jet P_T balancing). For jet P_T balancing, events were selected by requiring there be two and only two jets with $P_T > 15$ GeV/c, and that the azimuthal angle separating the two jets satisfy $150° < \Delta\phi < 210°$. The largest effect was for $M > 625$ GeV/c^2, where a 6% larger jet response at $|\eta| < 0.15$ and a 4% smaller jet response at $0.9 < |\eta| < 1.4$ produced a tilt in the Monte Carlo angular distribution that increased the relative rate at $\chi = 1$ by about 10% and lowered the relative rate at $\chi = 5$ by about 10%. We corrected both the χ and R_χ distributions for these and similar effects. The correction reduced R_χ by 1%, 2%, 3%, 5%, and 6% for the 5 mass bins, respectively. The correction increases with dijet invariant mass because the mass spectrum is steeper at higher mass values, leading to a larger distortion of the angular distribution.

In Figs. 1 and 2 and Tables I and II we present the corrected χ and R_χ distributions. The data are compared to the parton level predictions of leading order (LO) QCD, next to leading order (NLO) QCD from the JETRAD Monte Carlo program [15], and QCD plus a contact interaction. For the contact interaction curve, we normalized LO QCD plus a contact interaction to equal the NLO QCD predic-

tion with renormalization scale $\mu = P_T$ when the contact scale is $\Lambda = \infty$. This was done by multiplying the prediction, from LO QCD plus a contact interaction, by the ratio of the NLO to LO QCD predictions. The LO calculations use CTEQ2L parton distributions, and the NLO QCD calculation uses CTEQ2M parton distributions [16]. Alternate parton distribution sets were tried, including one in which the gluon distribution of the proton was significantly increased [4], and the calculations were insensitive to the choice of the parton distribution. In Fig. 2 the QCD calculations are shown for two different choices of renormalization scale, $\mu = M$ and $\mu = P_T$. The vertical axis in Fig. 2, R_χ, describes the shape of the angular distribution at a fixed mass, and is sensitive to the renormalization scale choice. The choice $\mu = M$ makes μ constant as a function of χ in a bin of fixed mass, while the choice $\mu = P_T$ requires μ to vary with χ. The renormalization scale dependence of the NLO calculation, which is significantly less than that of the LO calculation, provides an estimate of the uncertainty in the NLO QCD calculation. Figure 2 also illustrates that a contact interaction would cause R_χ to increase at high mass, while QCD calculations predict that R_χ is roughly 0.7 at all masses shown. The angular distributions and angular ratio are in good agreement with the NLO QCD prediction.

The systematic uncertainties, shown only in Fig. 2 and Table II, arise from the uncertainty in the jet energy response as a function of η. The response uncertainties are largest in the region $|\eta| < 0.15$ (between 3% and 6%) and the region $0.9 < |\eta| < 1.4$ (4%). Other systematic uncertainties are negligible in comparison. Since the systematic uncertainties are larger than the statistical uncertainties, a cross check was per-

formed to verify the integrity of the measurement. The uncorrected χ and R_χ distributions were remeasured with the detector pseudorapidity requirement $0.1 < |\eta| < 1.0$, eliminating the most problematic regions of the detector. The resulting uncorrected distributions were then corrected back to the standard region $|\eta| < 2$, using the same parametrized Monte Carlo program, and compared with the standard results. The corrected χ and R_χ distributions for the region $0.1 < |\eta| < 1.0$ agreed with those determined in the standard region $|\eta| < 2$ within the statistical uncertainties.

The systematic uncertainties on R_χ are highly correlated as a function of mass. The diagonal terms of the covariance matrix for the R_χ vs. mass distribution can be written as $V_{ii} = \sigma_i^2(stat)+\sigma_i^2(sys)$, and the off-diagonal terms are $V_{ij} = \sigma_i(sys)\sigma_j(sys)$, $i \neq j$, for mass bins i and j. Using this prescription and Table II the reader can reconstruct the full covariance matrix. We form a statistical comparison between the data and the theory by using the inverse of the covariance matrix, $(V^{-1})_{ij}$, and the difference between the data and the theory in each bin, Δ_i, to define $\chi^2 = \sum_{i,j} \Delta_i (V^{-1})_{ij} \Delta_j$. The resulting comparison between data and NLO QCD with renormalization scale $\mu = P_T$ is $\chi^2 = 8.36$ for 5 degrees of freedom. This is a better agreement than $\chi^2 = 13.1$ for NLO QCD with $\mu = M$.

We exclude at 95% CL any theoretical prediction which gives a χ^2 of greater than 11.1 when compared to our data. In a model of contact interactions where the up and down type quarks are composite we exclude at 95% CL the scales $\Lambda_{ud}^+ \leq 1.6$ TeV and $\Lambda_{ud}^- \leq 1.4$ TeV. For flavor symmetric contact interactions among all quark flavors [17], not just up and down quarks, the scales excluded by the angular distribution are

$\Lambda^+ \leq 1.8$ TeV and $\Lambda^- \leq 1.6$ TeV.

We compare these exclusions with the inclusive jet cross section analysis [3], where we reported a broad minimum in the χ^2 between data and the compositeness model for the scales $1.5 \leq \Lambda^+_{ud} \leq 1.8$ TeV, and best agreement for the scale $\Lambda^+_{ud} = 1.6$ TeV. Here we have excluded at 95% CL the portion of this broad minimum up to the scale $\Lambda^+_{ud} = 1.6$ TeV. The inclusive jet cross section χ^2 is sensitive to the choice of parton distributions while the dijet angular distribution χ^2 is not. The inclusive jet analysis used MRSD0′ parton distributions [18] with renormalization scale $\mu = E_T/2$. Changing the sign of the contact interaction from positive to negative produces a larger deviation of the composite model from QCD for the inclusive jet cross section, but produces a smaller deviation from QCD in the shape of the angular distribution. Therefore, if we had chosen to fit the inclusive jet cross section with the negative sign contact interaction, best agreement would have been found with less compositeness, corresponding to the larger scale $\Lambda^-_{ud} = 1.8$ TeV, which is not excluded by the angular distribution.

In conclusion, we have measured the dijet angular distributions and found them to be in good agreement with NLO QCD. We have presented limits on the left-handed contact interactions among quarks that could result if quarks were composite particles. Although the origin of the excess in the inclusive jet E_T spectrum has not been determined, the angular distribution data are consistent with the hypothesis that the high-E_T jet excess is caused by effects within the Standard Model. The angular distribution data exclude at the 95% CL the hypothesis that the high-E_T

jet excess is caused by a contact interaction among up and down quarks with scale $\Lambda_{ud}^{+} \leq 1.6$ TeV.

We thank the Fermilab staff and the technical staffs of the participating institutions for their vital contributions. This work was supported by the U.S. Department of Energy and National Science Foundation; the Italian Istituto Nazionale di Fisica Nucleare; the Ministry of Education, Science and Culture of Japan; the Natural Sciences and Engineering Research Council of Canada; the National Science Council of the Republic of China; and the A. P. Sloan Foundation.

References

[1] F. Abe *et al.*, Phys. Rev. Lett. **69**, 2896 (1992).

[2] E. Eichten, K. Lane, and M. Peskin, Phys. Rev. Lett. **50**, 811 (1983).

[3] F. Abe *et al.*, Phys. Rev. Lett. **77**, 438 (1996).

[4] J. Huston *et al.*, Phys. Rev. Lett. **77**, 444 (1996).

[5] H. L. Lai *et al.*, MSU-HEP-60426, hep-ph/9606399 (1996), submitted to Phys. Rev. D.

[6] S. Catani *et al.*, CERN-TH/96-85, hep-ph/9604351 (1996), to be published in Nucl. Phys. B.

[7] M. Bander, Phys. Rev. Lett. **77**, 601 (1996); K. Akama and H. Terazawa, INS-Rep-1154, hep-ph/9608279 (1996).

[8] G. Altarelli *et al.*, Phys. Lett. **B375**, 292 (1996); P. Chiappetta *et al.*, Phys. Rev. **D54**, 789 (1996).

[9] S. Chivukula *et al.*, Phys. Lett. **B380**, 92 (1996).

[10] L. Clavelli and I. Terekhov, Phys. Rev. Lett. **77**, 1941 (1996).

[11] D. Silverman, SLAC-PUB-7166, hep-ph/9605318 (1996), submitted to Phys. Rev. D.

[12] F. Abe *et al.*, Nucl. Instrum. and Meth. **A271**, 387 (1988).

[13] F. Abe *et al.*, Phys. Rev. D **45**, 1448 (1992).

[14] F. Abe *et al.*, Phys. Rev. Lett. **74**, 3538 (1995).

[15] W. Giele *et al.*, Phys. Rev. Lett. **73**, 2019 (1994).

[16] J. Botts *et al.*, Phys. Lett. **B304**, 159 (1993).

[17] K. Lane, BUHEP-96-8, hep-ph/9605257 (1996).

[18] A. D. Martin, R. G. Roberts, and W. J. Stirling, Phys. Lett. **B306**, 145 (1993).

Table I: The dijet angular distribution and statistical uncertainty for the five mass bins (GeV/c^2).

	(100/N)(dN/dχ)				
χ	$241 < M < 300$	$300 < M < 400$	$400 < M < 517$	$517 < M < 625$	$M > 625$
1.25	31.1 ± 0.7	31.7 ± 0.5	31.9 ± 0.5	32.6 ± 1.2	31.7 ± 2.4
1.75	26.8 ± 0.6	26.5 ± 0.5	26.3 ± 0.4	27.2 ± 1.1	26.5 ± 2.2
2.25	23.0 ± 0.6	23.8 ± 0.5	24.3 ± 0.4	25.1 ± 1.1	26.3 ± 2.2
2.75	23.4 ± 0.6	23.2 ± 0.5	23.9 ± 0.4	23.0 ± 1.0	25.3 ± 2.2
3.25	24.3 ± 0.7	23.8 ± 0.5	23.5 ± 0.4	21.2 ± 1.0	21.6 ± 2.0
3.75	22.5 ± 0.6	24.0 ± 0.5	23.3 ± 0.4	24.1 ± 1.1	22.2 ± 2.1
4.25	24.6 ± 0.8	23.3 ± 0.5	23.6 ± 0.5	22.8 ± 1.1	22.4 ± 2.1
4.75	24.4 ± 0.8	23.7 ± 0.5	23.1 ± 0.5	24.1 ± 1.2	24.0 ± 2.2

Table II: The mean dijet mass (GeV/c^2), number of events, dijet angular ratio R_χ, and its statistical and systematic uncertainty. The completely correlated systematic uncertainty can be used to form the covariance matrix (see text).

<Mass>	Events	R_χ	Stat.	Sys.
263	15023	0.678	0.012	0.018
334	23227	0.695	0.010	0.025
440	28202	0.703	0.009	0.033
557	4425	0.738	0.023	0.054
698	1056	0.732	0.046	0.103

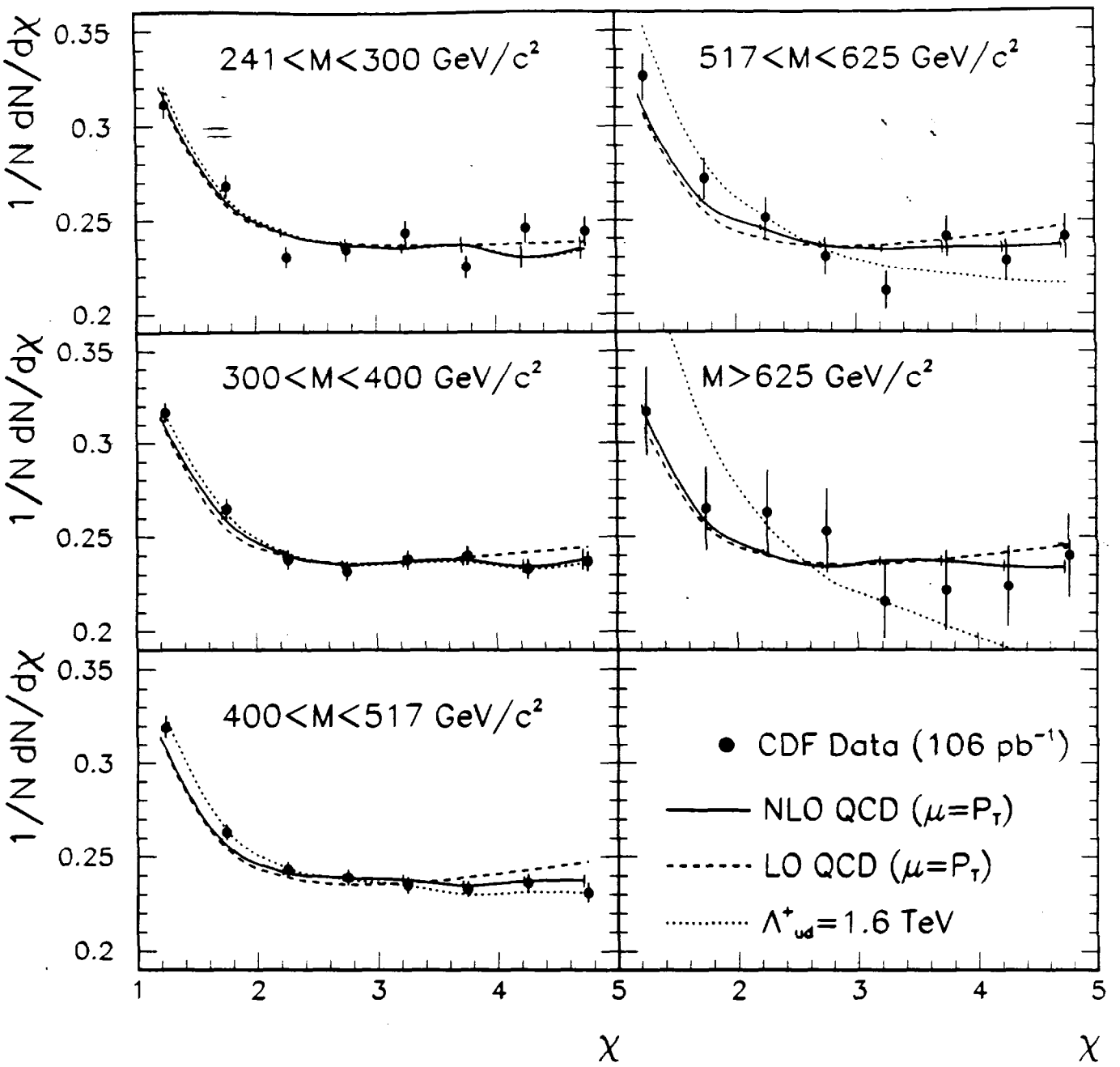

Figure 1: The dijet angular distribution (points) compared to predictions of NLO QCD (solid curve), LO QCD (dashed curve), and LO QCD with a quark contact interaction (dotted curve). The contact interaction calculation is normalized to equal NLO QCD when $\Lambda_{ud} = \infty$ (see text). Error bars on the data and NLO QCD are statistical.

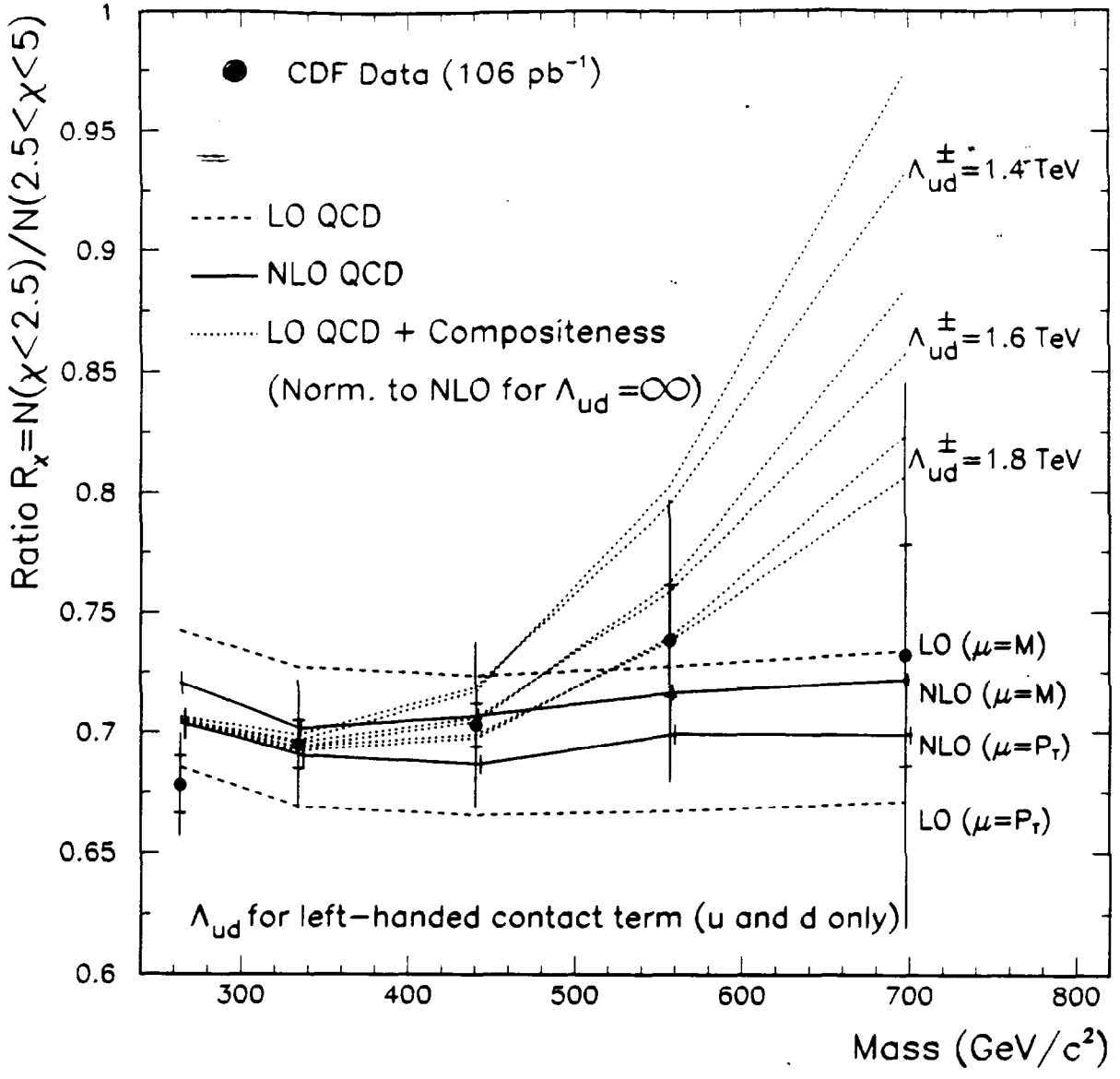

Figure 2: The dijet angular ratio (points) as a function of the dijet invariant mass, compared to LO QCD (dashed curve), NLO QCD (solid curve), and LO QCD with a quark contact interaction normalized to NLO at $\Lambda_{ud} = \infty$ (dotted curve). QCD is shown for two renormalization scales ($\mu = M$ and $\mu = P_T$). Contact interactions are displayed for three different compositeness scales, with two different signs for the amplitude of the contact term (upper dotted curve is Λ_{ud}^{+}, lower dotted curve is Λ_{ud}^{-}). The inner error bars on the data are statistical uncertainties and the outer error bars are statistical and systematic uncertainties added in quadrature. The error bars on NLO QCD are statistical.